

Flat Central Density Profile and Constant DM Surface Density in Galaxies from Scalar Field Dark Matter

Victor H. Robles^{*} and T. Matos[†]

Departamento de Física, Centro de Investigación y de Estudios Avanzados del IPN, AP 14-740, 0700 D.F., México

9 November 2021

ABSTRACT

The scalar field dark matter (SFDM) model proposes that galaxies form by condensation of a scalar field (SF) very early in the universe forming Bose-Einstein Condensates (BEC) drops, i.e., in this model haloes of galaxies are gigantic drops of SF. Here big structures form like in the Λ CDM model, by hierarchy, thus all the predictions of the Λ CDM model at big scales are reproduced by SFDM. This model predicts that all galaxies must be very similar and exist for bigger redshifts than in the Λ CDM model. In this work we show that BEC dark matter haloes fit high-resolution rotation curves of a sample of thirteen low surface brightness galaxies. We compare our fits to those obtained using a Navarro-Frenk-White and Pseudo-Isothermal (PI) profiles and found a better agreement with the SFDM and PI profiles. The mean value of the logarithmic inner density slopes is $\alpha = -0.27 \pm 0.18$. As a second result we find a natural way to define the core radius with the advantage of being model-independent. Using this new definition in the BEC density profile we find that the recent observation of the constant dark matter central surface density can be reproduced. We conclude that in light of the difficulties that the standard model is currently facing the SFDM model can be a worthy alternative to keep exploring further.

Key words: cosmology: dark matter – cosmology: observations – galaxies: fundamental parameters

1 INTRODUCTION

In the Λ Cold Dark Matter (Λ CDM or Λ CDM) model, known as the standard model of cosmology, the formation of structures in the universe is through a hierarchical process of growth of structures, meaning that small structures, like small haloes of galaxies merge to form bigger ones, like galaxy clusters and superclusters haloes. In this picture, the universe contains around 96 per cent of an unknown form of energy that is usually called dark matter (DM) and dark energy. The Λ CDM model can successfully describe cosmological observations such as the large scale distribution of galaxies, the temperature variations in the cosmic microwave background radiation and the recent acceleration of the universe (Coles 2005; Lahav & Liddle 2010; Peebles et al. 2009; Guo et al. 2011).

However, recent observations in far and nearby galaxies have shown that the model faces serious conflicts when trying to explain the galaxy formation at small scales (see Robles & Matos 2011 for a review; Friedmann 2011).

For instance, in the Λ CDM simulations the halos present rising densities towards the central region behaving as $\rho \sim r^{-1}$ well within 1 kpc (Navarro et al. 2010). On the other hand various observations suggest that the rotation curves are more consistent with a constant central density (Kuzio de Naray et al. 2008; de Blok 2010), this is most commonly known as the cusp/core problem (de Blok 2010).

Studying a wide range of galaxies of different morphologies and with magnitudes in the interval $-22 \leq M_B \leq -8$ Donato et al. (2009) fit their rotation curves (RC) using a Burkert profile for the DM (Burkert 1995) and found that

$$\log(\mu_0/M_\odot pc^{-2}) = 2.15 \pm 0.2 \quad (1)$$

remains approximately constant, where

$$\mu_0 = \rho_0 r_0 \quad (2)$$

with ρ_0 the central DM density and r_0 the core radius. Similar results were found in Kormendy & Freeman (2004); Spano et al. (2008). Exploring further the constant value of μ_0 for the DM, Gentile et al. (2009) found that within r_0 the DM central surface density in terms of the mass inside it ($M_{<r_0}$) is $< \Sigma_{>0,DM} = M_{<r_0}/\pi r_0^2 \approx 72^{+42}_{-27} M_\odot pc^{-2}$, the gravitational acceleration due to DM felt by a test particle

^{*} E-mail: vrobles@fis.cinvestav.mx

[†] E-mail: tmatos@fis.cinvestav.mx

at the radius r_0 was found to be

$$g_{DM}(r_0) = G\pi < \Sigma >_{>0,DM} = 3.2_{-1.2}^{+1.8} \times 10^{-9} \text{ cm s}^{-2}, \quad (3)$$

additionally they reported the acceleration due to the luminous matter at r_0 to be $g_{bar}(r_0) = 5.7_{-2.8}^{+3.8} \times 10^{-10} \text{ cm s}^{-2}$.

In the Λ CDM model the galaxies have evolved through numerous mergers and grown in different environments, the star formation and basic properties of the galaxies are not expected to be a common factor among them. Therefore explaining both the constancy of μ_0 and the core in the central regions of galaxies seems very unlikely in this model.

These problems can be used to test alternative DM models. There are other models that do not include DM but instead modify the Newtonian force law $\mathbf{F} = m\mathbf{a}$, one of them is called MOND and was proposed by Milgrom (Milgrom 2010; Sanders 2009), in this modification Newton's law reads $\mathbf{F} = m\mathbf{a}\mu(a/a_0)$, where the fixed acceleration scale a_0 divides the Newtonian and MONDian regimes, for $x \ll 1$ $\mu(x) = x$ we have the MONDian regime and for $x \gg 1$ we recover the usual Newtonian acceleration, the value of $a_0 \sim 1.2 \times 10^{-10} \text{ m/s}^2$.

Lately, the scalar field dark matter (SFDM) model has received much attention. When the scalar field contains a self-interaction this model is also called the Bose-Einstein Condensate (BEC) dark matter model, both names are used in the literature and are interchangeable. The main idea is simple (Guzmán & Matos 2000). The SFDM model proposes that galaxies form by condensation of a scalar field (SF) with an ultra-light mass of the order of $m_\phi \sim 10^{-22} \text{ eV}$. Therefore, when we mention the SFDM or BEC model in this paper we are describing a scalar field that condensates somehow and becomes Bose Einstein Condensate dark matter. From this mass it follows that the critical temperature of condensation $T_c \sim 1/m_\phi^{5/3} \sim \text{TeV}$ is very high, thus, they form Bose-Einstein Condensates (BEC) drops very early in the universe. It has been proposed that these drops are the haloes of galaxies (see Matos & Ureña 2001), *i.e.*, that haloes are gigantic drops of SF. On the other side, big structures form like in the LCDM model, by hierarchy (Matos & Ureña 2001; Suárez & Matos 2011), thus, all predictions of the LCDM model at big scales are reproduced by SFDM. In other words, in the SFDM model the haloes of galaxies do not form hierarchically, they form at the same time and in the same way when the universe reaches the critical temperature of condensation of the SF, in a similar way as water drops form in the clouds. From this it follows that all galaxies must be very similar because they formed in the same manner and at the same moment. Therefore, from this model we have to expect that there exist well formed galaxy haloes at bigger redshifts than in the LCDM model. In this model the scalar particles with this small mass are such that their wave properties avoid the cusp and reduce the high number of small satellites (Hu, Barkana & Gruzinov 2000) which is another problem that is still present in the Λ CDM model (see Robles & Matos 2011 for a review; Klypin et al. 1999). Summarizing, it is remarkable that with only one free parameter, the ultra-light scalar field mass ($m_\phi \sim 10^{-22} \text{ eV}$), the SFDM model fits:

(i) The evolution of the cosmological densities (Matos, Vazquez & Magaña 2009).

(ii) The rotation curves of big galaxies (Harko 2011a; Bernal et al. 2008) and LSB galaxies.

(iii) With this mass, the critical mass of collapse for a real scalar field is just $10^{12} M_\odot$, *i.e.*, the one observed in galaxy haloes (Alcubierre et al. 2002).

(iv) The scalar field has a natural cut off, thus the substructure in clusters of galaxies is avoided naturally. With a scalar field mass of $m_\phi \sim 10^{-22} \text{ eV}$ the amount of substructure is compatible with the observed one (Matos & Ureña 2001; Suárez & Matos 2011).

(v) We expect that SFDM forms galaxies earlier than the cold dark matter model, because they form BECs at a critical temperature $T_c \gg \text{TeV}$. So if SFDM is right, we have to see big galaxies at big redshifts with similar features.

(vi) And recently it has been demonstrated that SFDM haloes maintain satellite galaxies going around big galaxies for enough time to explain the existence of old stars in the satellites, provided that the mass of the SF is just $m_\phi \sim 10^{-22} \text{ eV}$ (Lora et al. 2011).

The idea was first considered by Sin (1994); Ji S. U. & Sin S. J. (1994) and independently introduced by Guzmán & Matos (2000). In the BEC model, DM halos can be described in the non-relativistic regime, where DM halos can be seen as a Newtonian gas. If we consider a SF self-interaction, we need to add a quartic term to the SF potential, in this case the equation of state of the SF is that of a polytropic of index $n=1$ (Suárez & Matos 2011; Harko 2011a). Different issues of BEC DM halos and the cosmological behavior of the BEC model have been studied in Colpi et al. (1986); Gleiser et al. (1988); Bohmer & Harko (2007); Harko (2011a); Matos & Guzmán (2001); Chavanis (2011).

It is a fact that any model trying to become a serious alternative to Λ CDM has to succeed not only in reproducing observations in which the standard model fails but also has to keep the solid description at large scale. For this reason, our aim in this work is to test the BEC model with the two observations mentioned above, the cusp/core problem (Bohmer & Harko 2007) and the constant DM central surface density. In order to do this, we used the Thomas-Fermi approximation and a static BEC DM halo to fit rotation curves of a set of galaxies. However, so far there was no comparison between the density profile and the data, in this work we fill this blank by fitting rotation curves of 13 high resolution low surface brightness (LSB) galaxies and additionally compare the fits to two characteristic density profiles 1) the cuspy Navarro-Frenk-White (NFW) profile that results from N-body simulations using Λ CDM and 2) the Pseudo Isothermal (PI) core profile. The comparison allow us to show that the model is in general agreement with the data and with a core in the central region. For our second result we found that the meaning of a core is somewhat ambiguous. In order to clarify the meaning and unify the description, we propose a new definition for the core and core radius that allow us to decide when a density profile is cusp or core. Using this definition in the BEC model discussed above we find that the BEC model can reproduce the constant value of μ_0 and as a crosscheck we used the PI profile and find our results to be in very good agreement with observations. This argues in favor of the model and our definition.

In section 2, we describe the density profiles we use to fit the rotation curves and we give our definition of the core

and core radius. In section 3, we fit the galaxy data and obtain the fitting parameters and the core radius for the PI and BEC density profiles. In section 4, we discuss our results and in section 5 we give our conclusions.

2 DARK MATTER HALO DENSITY PROFILES

In this section we provide the dark matter profiles that will be used in the analysis. In the last part of the section we briefly describe the usual meaning of the core and establish a new definition for it.

2.1 BEC profile

The case in which the dark matter is in the form of a static Bose-Einstein condensate and the number of DM particles in the ground state is very large was considered in Bohmer & Harko (2007). Following this paper and assuming the Thomas-Fermi approximation (Dalfovo et al. 1999) which neglects the anisotropic pressure terms that are relevant only in the boundary of the condensate, the system of equations describing the static BEC in a gravitational potential V is given by

$$\nabla p \left(\frac{\rho}{m} \right) = -\rho \nabla V \quad (4)$$

$$\nabla^2 V = 4\pi G \rho, \quad (5)$$

with the following equation of state

$$p(\rho) = U_0 \rho^2, \quad (6)$$

where $U_0 = \frac{2\pi\hbar^2 a}{m^3}$, ρ is the mass density of the static BEC configuration and p is the pressure, as we are considering zero temperature p is not a thermal pressure but instead it is produced by the strong repulsive interaction between the ground state bosons. Assuming spherical symmetry and denoting R as the radius at which the pressure and density are zero, the density profile takes the form (Bohmer & Harko 2007)

$$\rho_B(r) = \rho_0^B \frac{\sin(kr)}{kr} \quad (7)$$

where $k = \sqrt{Gm^3/\hbar^2 a} = \pi/R$ and $\rho_0^B = \rho_B(0)$ is the BEC central density, m is the mass of the DM particle and a is the scattering length. The mass at the radius r is given by

$$m(r) = \frac{4\pi\rho_0^B}{k^2} r \left(\frac{\sin(kr)}{kr} - \cos(kr) \right), \quad (8)$$

from here the tangential velocity V_B of a test particle at a distance r , is

$$V_B^2(r) = \frac{4\pi G \rho_0^B}{k^2} \left(\frac{\sin(kr)}{kr} - \cos(kr) \right). \quad (9)$$

The logarithmic slope of a density profile is defined as

$$\alpha = \frac{d(\log \rho)}{d(\log r)} \quad (10)$$

using (7) in (10) it is obtained (Harko 2011b)

$$\alpha(r) = - \left[1 - \frac{\pi r}{R} \cot \left(\frac{\pi r}{R} \right) \right]. \quad (11)$$

Additionally, the logarithmic slope of the rotation curve is defined (Harko 2011b) by

$$\beta = \frac{d(\log V)}{d(\log r)} \quad (12)$$

from (9) we get

$$\beta = -\frac{1}{2} \left[1 - \frac{(\pi r/R)^2}{1 - (\pi r/R) \cot(\pi r/R)} \right]. \quad (13)$$

2.2 Pseudo Isothermal profile

All the empirical core profiles that exist in the literature fit two parameters, a scale radius and a scale density. A characteristic profile of this type is

$$\rho_{PI} = \frac{\rho_0^{PI}}{1 + (r/R_c)^2}, \quad (14)$$

this is the PI profile (Begeman et al. 1991). Here R_c is the scale radius and ρ_0^{PI} is the central density. The rotation curve is

$$V(r)_{PI} = \sqrt{4\pi G \rho_0^{PI} R_c^2 \left(1 - \frac{R_c}{r} \arctan \left(\frac{r}{R_c} \right) \right)}. \quad (15)$$

2.3 Navarro-Frenk-White profile

The NFW profile emerges from numerical simulations that use only CDM and are based on the Λ CDM model (Dubinski et al. 1991; Navarro et al. 1996, 1997). In addition to this, we have chosen this profile because it is representative of what is called the cuspy behavior ($\alpha \approx -1$) in the center of galaxies due to DM. The NFW density profile (Navarro et al. 1997) and the rotation curve are given respectively by

$$\rho_{NFW}(r) = \frac{\rho_i}{(r/R_s)(1 + r/R_s)^2} \quad (16)$$

$$V_{NFW}(r) = \sqrt{4\pi G \rho_i R_s^3} \sqrt{\frac{1}{r} \left[\ln \left(1 + \frac{r}{R_s} \right) - \frac{r/R_s}{1 + r/R_s} \right]}, \quad (17)$$

ρ_i is related to the density of the universe at the moment the halo collapsed and R_s^2 is a characteristic radius.

2.4 Meaning of the core radius and cusp/core discrepancy

In the large scale simulations that use collisionless cold dark matter the inner region of DM halos show a density distribution described by a power law $\rho \sim r^\alpha$ with $\alpha \approx -1$, such behaviour is what is now called a cusp. On the other hand, observations mainly in dwarf and LSB galaxies seem to prefer a central density going as $\rho \sim r^0$. This discrepancy between observation and the CDM model receives the name of cusp/core problem. Among the empirical profiles most frequently used to describe the constant density behavior in these galaxies are the PI (Begeman et al. 1991), the isothermal (Athanasoula et al. 1987) and the Burkert profile (Burkert 1995). Even though their behavior is similar in the central region and is specified by the central density fitting parameter, their second parameter called the core

radius does not represent the same idea. For instance, in the PI profile (eq.(14)) we see that the core radius will be the distance in which the density is half the central density. For the Burkert profile the core radius R_c^{burk} will be when $\rho^{burk}(R_c^{burk}) = \rho_0^{burk}/4$ and for an isothermal profile (I) (Spano et al. 2008) $\rho^I(R_c^I) = \rho_0^I/2^{3/2}$. Hence, we see an ambiguity in the meaning of the core radius, they get the same name but the interpretation depends on the profile. If we want to compare the central density of LSB galaxies with that of NFW, it usually suffice to have a qualitative comparison, so far this is what we have been doing by fitting empirical profiles. However, high resolution rotation curves demand a more quantitative comparison. Indeed, if we want to test models by fitting RCs we have to know the specific meaning and size of the core, then we will be able to tell if a model is consistent with a cusp or not by making a direct comparison with the data.

For this reason we ask ourselves the question: *What and where is the core?* To solve the previous ambiguity and to unify the concept for future comparisons, we found that a good definition for the *core* is a region where the density profile presents logarithmic slopes $\alpha \geq -1$ and the core radius will be the radius at which the core begins, that is to say, for radius smaller than the core radius we will have $\alpha \geq -1$, this means that its value r' is determined by the equation

$$\alpha(r') = -1 \quad (18)$$

The advantages of this definition are that the interpretation is independent of the profile chosen (also notice that it applies to the total density profile and is not restricted to that of DM) and in virtue of the same definition we can directly tell if a DM model profile is cored or cuspy. With our new definition the specific distance at which the core radius occurs still depends on the profile chosen but now the physical interpretation is only one. In the following when we refer to both the core and core radius we adopt the previous interpretation.

Applying the definition to (7) we get the core radius for the BEC profile R_B and for comparison we use (14) because in turns out that the parameter R_c corresponds to the core radius as defined above. Finally, fitting the NFW profile provides a direct comparison between a cusp and core and hence to the cusp/core problem.

3 FITS AND DATA

We see from (7) that the BEC model satisfies $\rho \sim r^0$ near the origin, but a priori this does not imply consistency with observed RCs. Therefore, we fit the profiles in section 2 to thirteen high resolution observed RCs of a sample of LSB galaxies. The RCs were taken from a subsample of de Blok et al. (2001), we chose galaxies that have at least 3 values within ~ 1 kpc, not presenting bulbs and the quality in the RC in $H\alpha$ is good as defined in McGaugh S. S. et al. (2001). The RCs in this work omit galaxies presenting high asymmetries and included in the error bars are experimental errors in the velocity measurement, inclination and small asymmetries. Because the DM is the dominant mass component for these galaxies we adopt the minimum disk hypothesis which neglects baryon contribution to the observed RC. In order to show that in LSB and dwarf galaxies neglecting the effect of

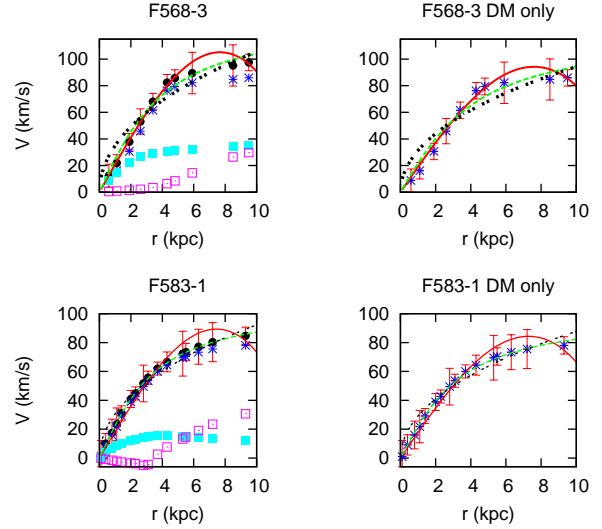


Figure 1. Contribution of the baryons to the rotation curve for F568-3 and F583-1. We denote observed data by black dots with error bars, dark matter with blue asterisks, the disk with cyan squares and the gas with magenta squared boxes. We fit the figures on the left assuming the minimum disk hypothesis while for the ones on the right we subtract in quadrature the baryons and fit only the dark matter. We notice that the barionic component is not dominant in the outer regions and that the difference in the fits is barely noticeable.

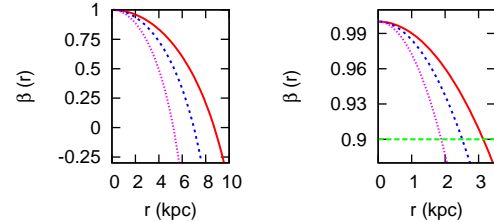
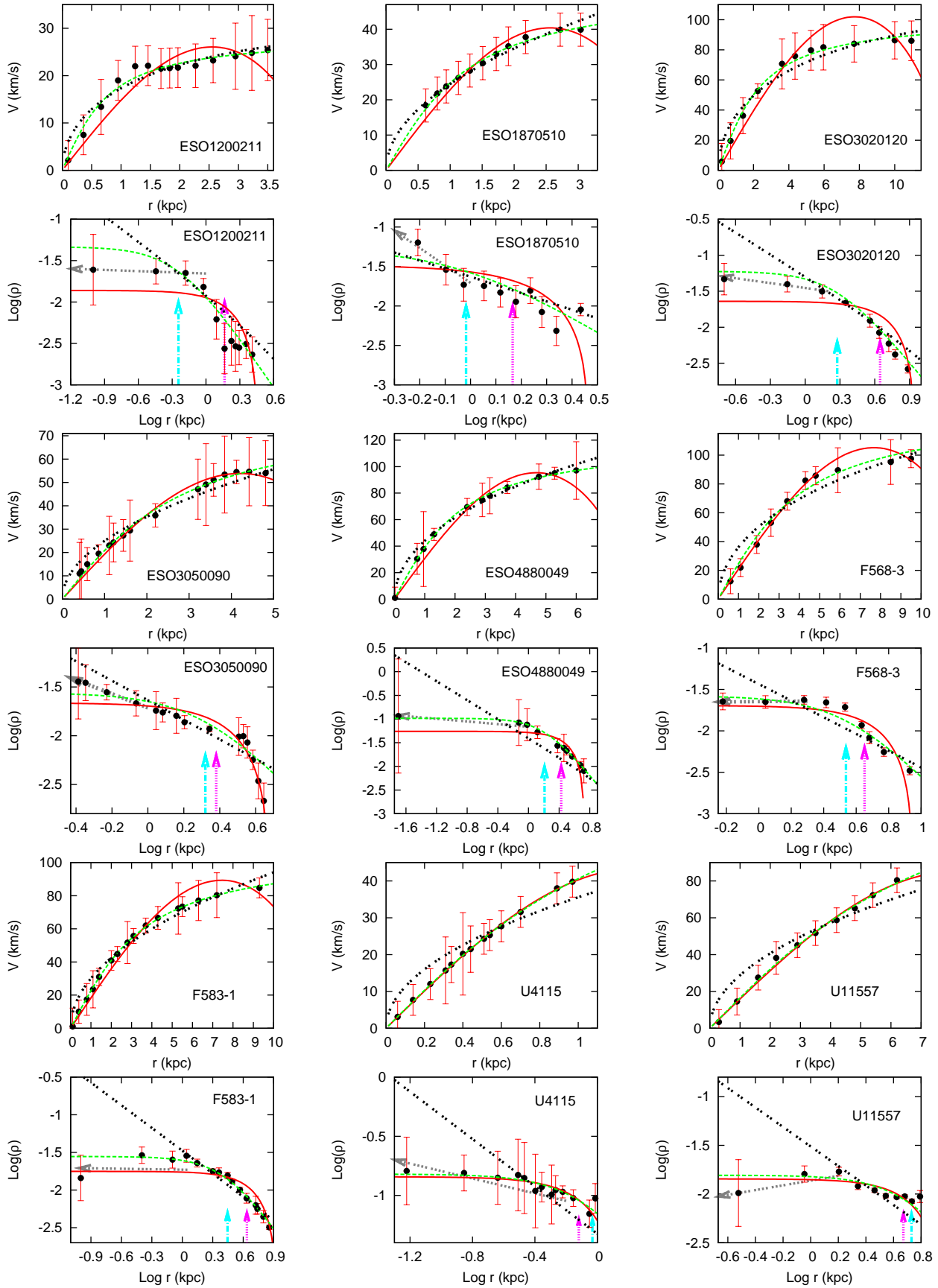


Figure 2. Logarithmic slope of the rotation curve (β) for three values of R . From left to right $R = 6, 8, 10$. The plots on the left show a common behavior always reaching zero before R . The figure on the right shows the region where a linear behavior in the RC speed is still valid, the (green) horizontal line bounds this region and the radius in which this boundary is reached was found to be $r \approx 0.31R$ in each curve.

baryons is a good hypothesis, we include in Fig.1 two representative examples (F568-3 and F583-1). For these galaxies we plot the contribution of the gas, disk and the dark matter separately. We did the fitting first considering the total contribution and then using only DM (marked as 14 and 15 in Table 1 and 2). We found no substantial difference in our values, which can be seen from our results in Table 1 and 2. As the other galaxies belong to the category of DM dominated galaxies as other authors have shown (Kuzio de Naray et al. 2008; de Blok et al. 2001), neglecting baryons in our analyses will not modify substantially our results.

As the difference between a core and a cusp is most notable only for data values inside 1 kpc and given that in the interval ~ 1 to 10 kpc the slopes of core and cusp profiles are very similar, which can lead to the wrong conclusion that cuspy halos are consistent with observations, we deter-



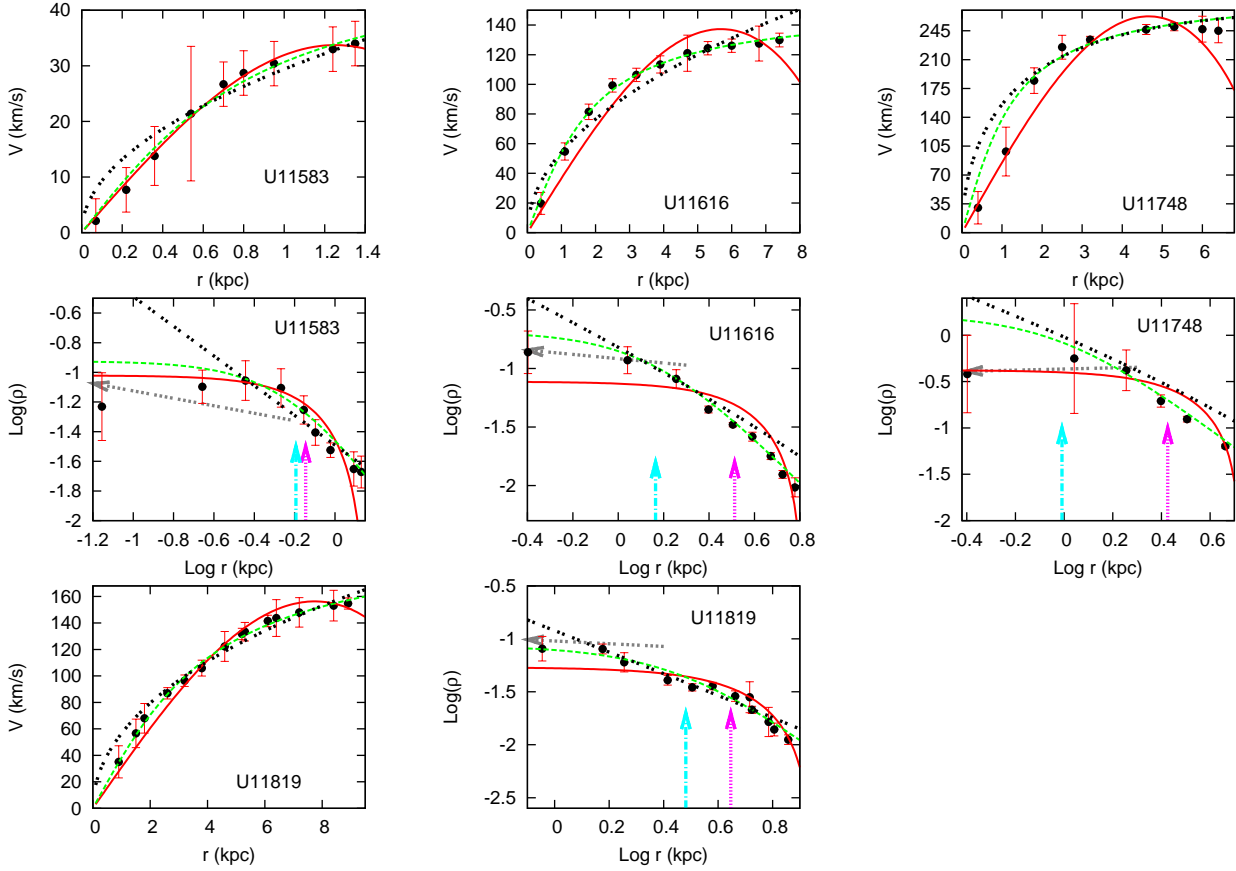


Figure 3. Observed LSB galaxy rotation curves and density profiles with the best halo fits. Below each RC is its density profile along with the fits. Shown are the PI (green dashed-line); the BEC (red solid line) and NFW (black double-dotted line) DM halo profiles, the observational data is drawn with error bars. The gray arrow denotes the best fit to the data within R_1 and the vertical arrows denote the PI (blue) and BEC (magenta) core radius.

mined the logarithmic slope and the uncertainty following de Blok et al. (2001) with the difference that we fit only the data within 1 kpc and that there is no need of an uncertain “break radius”.

In Table 1 we list the fitting parameters of the profiles of section 2, we also include the values of the logarithmic slope and its uncertainty, the value R_1 denotes the nearest radius to 1kpc where a data point is given. We obtain α by fitting values inside R_1 , and we also report the core radius for the BEC profile R_B in order to compare it with R_c . In Table 2 we report both the value of eq. (3) for the BEC profile and the logarithm of eq. (2) for PI and BEC profiles.

In Fig. 3, we show our fits to the RC data and the density profiles, also shown are the core radius in the BEC (magenta) and in PI (blue) profiles. The gray arrow is the fit that determines α , the size of the arrow denotes the fitted region and is bounded by R_1 .

4 DISCUSSION

In Fig. 2 we plot β using three different values of R . From this figure we see a common behavior. We have that β is a decreasing function of r and is zero before R , which tell us that (9) always reaches a maximum before R . We also notice that there is a region in which $V_B \sim r$, we can take this region to be when $0.9 \leq \beta \leq 1$. If we use $\beta = 0.9$ as

an upper bound for the region in which the linear behavior ($V_B \sim r$) remains valid, we obtain an upper bound radius of $r \approx 0.31R$. This means that for values of $r \leq 0.31R$ we expect $V_B \sim r$. The latter can be used as a test to the BEC model by fitting the RCs and verifying this solid-body behavior within the mentioned region. The fits of the RCs in Fig. 3 prove that the solid-body like behavior characterized by a linear increase of the velocity in the central region is satisfied by the BEC model, in fact, it is more consistent with the core PI and BEC profiles than the cuspy NFW.

If we now turn to the density profiles, our fits within R_1 give an average value of $\alpha = -0.27 \pm 0.18$ consistent with those obtained in de Blok et al. (2001) $\alpha = -0.2 \pm 0.2$ and with $\alpha = -0.29 \pm 0.07$ reported by Oh Se-Heon et al. (2011) analyzing 7 THINGS dwarf galaxies. The case of ESO1870510 might be considered to be consistent with NFW profile, however it is the innermost value that considerably decreases α , being an irregular galaxy more central data near the innermost region is required to discard the possibility of any violent event that might have caused such a slope value.

The density profiles corresponding to the RCs fits are also shown in Fig.3 for each galaxy. We see that the BEC fits slightly deviates for the farthest data points as a result of the finite size of the radius R that is fixed by the same data. This discrepancy is due to the fact that the halo might be more extended than the value R . As a matter of

Table 1. Best-fit parameters of the profiles in section 2.

(a)

Label	Galaxy	ρ_0^{PI} ($M_\odot pc^{-3}$)	R_c (kpc)	χ_{PI}^2	ρ_0^B ($M_\odot pc^{-3}$)	R (kpc)	R_B (kpc)	χ_B^2
1	ESO1200211	0.0464	0.57	1.45	0.0138	2.92	1.46	0.44
2	ESO1870510	0.0548	0.96	0.63	0.0329	2.93	1.465	0.2
3	ESO3020120	0.0598	1.89	0.03	0.0229	8.95	4.425	0.92
4	ESO3050090	0.0276	2.09	0.04	0.0217	4.81	3.04	0.1
5	ESO4880049	0.1035	1.62	0.99	0.0549	5.36	2.68	0.79
6	U4115	0.1514	0.93	0.10	0.1438	1.52	0.76	0.15
7	U11557	0.0156	5.37	0.08	0.0143	9.38	4.69	0.07
8	U11611	0.2065	1.46	0.14	0.0771	6.51	3.225	5.24
9	U11748	1.678	0.98	1.43	0.4205	5.33	2.665	4.37
10	U11819	0.0869	3.03	0.20	0.0539	8.86	4.43	1.09
11	U11583	0.119	0.64	0.12	0.0953	1.43	0.715	0.84
12	F568-3	0.0361	3.01	0.53	0.0248	8.78	4.39	0.11
13	F583-1	0.0317	2.6	0.54	0.019	8.53	4.26	0.48
14	F568-3 (DM)	0.0264	3.44	0.84	0.0202	8.96	4.48	0.25
15	F583-1 (DM)	0.0279	2.79	0.58	0.0177	8.66	4.33	0.37

(b)

Label	Galaxy	ρ_i ($\times 10^{-3} M_\odot pc^{-3}$)	R_s (kpc)	χ_{NFW}^2	α	$\Delta\alpha$	R_1 (kpc)
1	ESO1200211	2.45	5.7	0.24	-0.04	0.53	0.95
2	ESO1870510	0.761	31.82	0.05	-1.09	0.76	1.13
3	ESO3020120	2.65	19.72	0.32	-0.2	0.16	1.4
4	ESO3050090	0.0328	705.67	0.22	-0.7	0.03	1.1
5	ESO4880049	1.42	52.27	0.16	-0.09	0.06	0.96
6	U4115	0.139	341.74	0.78	-0.27	0.24	0.89
7	U11557	0.0108	2849.65	1.43	0.2	0.31	0.9
8	U11611	11.59	14	1.77	-0.15	0.31	1.1
9	U11748	204.58	5.53	3.41	-0.38	0.11	1.1
10	U11819	1.19	101.24	1.07	-0.64	0.13	2.5
11	U11583	0.136	238.568	0.81	-0.2	0.24	0.95
12	F568-3	0.378	120.78	2.36	0.03	0.02	1.9
13	F583-1	0.345	102.349	0.55	-0.03	0.04	1.1
14	F568-3 (DM)	0.0715	515.68	2.87	0.34	0.27	1.9
15	F583-1 (DM)	0.329	102.349	0.58	0.02	0.07	1.1

a fact, the more extended the “flat” outer region in the RCs the more conspicuous the discrepancy. The main reason of this comes from Fig.2 where we infer that the rotation curve speed always presents a maximum value followed by a continuous decrease, which means that to avoid the mentioned discrepancy we need that the BEC rotation curve profile remains approximately constant after its maximum. From Fig.1 we see that the total rotation curve is dominated by the dark matter contribution, specially in the outer regions. Hence, unless the baryons become the dominant component in the outer regions, which does not seem to be observed, it is unlikely that adding the barionic contribution to the RCs in our galaxies will solve the discrepancy.

Some solutions to keep the BEC rotation curve constant after its maximum include finite temperature corrections to (14) (Harko & Madarassy 2011), this suffice to alleviate the latter problem in LSB galaxies and dwarfs but not for bigger galaxies. Other authors proposed including vortex lattices (Rindler-Daller & Shapiro 2011; Zinner 2011) and adding more nodes (Sin 1994; Ji S. U. & Sin S. J. 1994)

in the solution of system (4) and (5). Nevertheless, it can be shown (Guzmán & Ureña-López 2003) that a systems of many nodes is unstable, therefore so far no final conclusion has been reached.

When comparing the BEC and PI core radius we find a general difference of ~ 2 kpc, the core size in the PI profile is approximately 2 kpc smaller than the BEC core size, but the PI central density is larger. In U4115, U11557 and U11583 both profiles are very similar which results in a similar core and central density values, this can also be taken as a consistency check for our core definition.

Comparing the values of R_B in Table 1 we did not find a tendency to a common value. Assuming that the core radius determines the transition where the DM distribution changes from the outer region to the inner constant central density, the lack of a unique value means that there is not a common radius at which this transition takes place.

For our second test we use R_B to calculate (2). We have already seen that R_c and R_B are generally different and R_B is not a fit parameter. Hence *a priori* R_B is not expected to

Table 2. Derived quantities from the parameters in Table 1.

Label	Galaxy	$\log \mu_0^{PI}{}^a$	$\log \mu_0^B$	g_{DM}^B ($\times 10^{-9} \text{ cm s}^{-2}$)
1	ESO1200211	1.42 ± 0.13	1.60 ± 0.50	0.908
2	ESO1870510	1.72 ± 0.78	1.68 ± 0.58	2.15
3	ESO3020120	2.05 ± 0.52	2.00 ± 0.51	2.17
4	ESO3050090	1.76 ± 0.59	1.81 ± 0.60	4.58
5	ESO4880049	2.22 ± 0.11	2.16 ± 1.16	6.63
6	U4115	2.14 ± 0.40	2.03 ± 0.23	4.93
7	U11557	1.92 ± 0.31	1.82 ± 0.54	3.03
8	U11611	2.97 ± 0.13	2.40 ± 0.42	11.3
9	U11748	3.21 ± 1.98	3.05 ± 0.78	50.4
10	U11819	2.42 ± 0.30	2.37 ± 0.25	10.8
11	U11583	1.88 ± 0.25	1.83 ± 0.53	3.08
12	F568-3	2.03 ± 0.35	2.03 ± 0.53	4.91
13	F583-1	1.91 ± 0.23	1.91 ± 0.65	3.66
14	F568-3 (DM)	1.95 ± 0.51	1.95 ± 0.68	4.09
15	F583-1 (DM)	1.89 ± 0.13	1.88 ± 0.59	3.45

^a Both μ_0^{PI} and μ_0^B units are M_\odot/pc^2

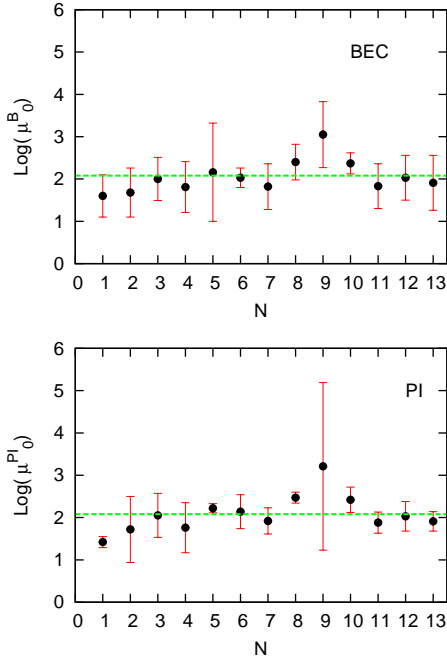


Figure 4. Plot of $\log(\mu_0^B/M_\odot\text{pc}^{-2})$ and $\log(\mu_0^{PI}/M_\odot\text{pc}^{-2})$ for each galaxy. N denotes the galaxy according to Table 1. Here we observe that these values remain approximately constant in both profiles, this also serves as a crosscheck for our definition of R_B in the BEC profile. The green dashed-line represents the mean values given in (19) and (20).

correlate with ρ_0^B . However, with the values of Table 1 we obtain

$$\log(\mu_0^B/M_\odot\text{pc}^{-2}) = \log \rho_0^B R_B = 2.05 \pm 0.56 \quad (19)$$

$$\log(\mu_0^{PI}/M_\odot\text{pc}^{-2}) = \log \rho_0^{PI} R_c = 2.08 \pm 0.46 \quad (20)$$

for the average values in the BEC and PI profiles respectively. We see the excellent agreement of (19) with (20) that

was used as a crosscheck and with (1) in which a much bigger sample was used. The agreement has shown that the BEC model is capable of reproducing the constancy of the value μ_0 , something that because of the cuspy nature is not possible in the NFW profile.

In Fig. 4 we plot the above values for each galaxy. We define the DM central surface density (mentioned in the introduction) for the BEC profile by

$$\langle \Sigma \rangle_{0,DM}^B = M_{<R_B} / \pi R_B^2, \quad (21)$$

where $M_{<R_B}$ is obtained from (8) evaluated at R_B . From Table 2 we see that for U11748 the value $\log \mu_0^{B,PI}$ is considerably above the rest and with the largest uncertainty. For this reason, in the following analysis we omit both, this value and the smallest one that corresponds to ESO1200211. Doing this we get an average value of eq. (19) given by $\langle \langle \Sigma \rangle_{0,DM}^B \rangle \approx 191.35 M_\odot\text{pc}^{-2}$, and for the acceleration felt by a test particle located in R_B due to DM only we have $g_{DM}(R_B) \approx 5.2 \times 10^{-9} \text{ cm s}^{-2}$ broadly consistent with (3).

The fact that all galaxies present approximately the same order of magnitude in $g_{DM}(R_B)$ might suggest that R_B represents more than a transition towards a constant density, it can give us information about the close relation between DM and the baryons. Moreover, in view of the lack of a unique core radius, we can interpret the transition in DM distribution as an effect of crossing a certain acceleration scale instead of a radial length scale. Such interpretation reminds us that given in MOND but with the big difference that the acceleration scale found is for DM and is not a postulate of the model.

To determine which interpretation causes the transition whether an acceleration scale or a length scale we will need to study the properties of larger samples of galaxies observed with the new telescopes.

5 CONCLUSIONS

In this paper we find that the BEC model gives a constant density profile that is consistent with RCs of dark matter dominated galaxies. The profile is as good as one of the most frequently used empirical core profiles but with the advantage of coming from a solid theoretical frame. We fit data within 1 kpc and found a logarithmic slope $\alpha = -0.27 \pm 0.18$ in perfect agreement with a core. It is important to notice that the cusp in the central regions is not a prediction that comes from first principles in the CDM model, it is a property that is derived by fitting simulations that use only DM.

We established the ambiguity present in the usual interpretation of the core radius, we proposed a new definition for the core and core radius that takes away the ambiguity and that has a clear meaning that allows for a definite distinction when a density profile is core or cusp.

Using our definition we find the core radius in the BEC profile to be in most cases over 2 kpc bigger than the core radius in the PI profile. We have assumed the DM particles are bosons and that a great number of them is in the ground state in the form of a condensate. This led us to good results for our sample of galaxies, but it might be necessary to consider more than these simple hypotheses.

As a second result and direct consequence of our core definition, we were able to obtain the constant value of μ_0 which is proportional to the central surface density. This result is one of several conflicts that jeopardize the current standard cosmological model.

If we continue to observe even more galaxies with a core behavior, this model can be a good alternative to Λ CDM.

ACKNOWLEDGMENTS

This work was partially supported by CONACyT México under grants CB-2009-01, no. 132400 and I0101/131/07 C-234/07 of the Instituto Avanzado de Cosmología (IAC) collaboration (<http://www.iac.edu.mx/>).

REFERENCES

- Alcubierre M., Siddhartha Guzmán F., Matos T., Núñez D., Ureña L. A., Wiederhold P., 2002, *Class. Quant. Grav.*, 19, 5017
- Athanassoula E., Bosma A., Papaioannou S., 1987, *A&A*, 179, 2340
- Begeman K. G., Broeils A. H., Sanders R. H., 1991, *MNRAS*, 249, 523
- Bernal A., Matos T., Núñez D., 2011, *Rev. Mex. A.A.*, 44, 149
- Bohmer C. G., Harko T., 2007, *JCAP06 (2007)*, 025
- Burkert A., 1995, *ApJ*, 447, L25
- Chavanis P. H., 2011, *Phys. Rev. D*, 84, 043531; *Phys. Rev. D* 84, 043532
- Coles P., 2005, *Nature*, 433, 248
- Colpi M., Shapiro S. L. and Wasserman I., 1986, *Phys. Rev. Lett.*, 57, 2485
- Dalfovo F., Giorgino S., Pitaevskii L. P., Stringari S., 1999, *Rev. Mod. Phys.* 71, 463

- de Blok W.J.G., 2010, *Adv. Astron.*, 2010, Article ID 789293, 14 pages.
- de Blok W. J. G. et al., 2001, *ApJ*, 552, L23
- Donato et al., 2009, *MNRAS*, 397, 1169
- Dubinski J., Carlberg R. G., 1991, *ApJ*, 378, 496
- Friedmann D. E., 2011, arXiv:0912.1668v4
- Gentile G., Famaey B., Zhao H., Salucci P., 2009, *Nature*, 461, 627
- Gleiser M., 1988, *Phys. Rev. D*, 38, 2376
- Guo, Q. et al., 2011, *MNRAS*, 413, 101
- Guzmán F. S., Matos T., 2000, *Class. Quant. Grav.*, 17, L9
- Guzmán F.S., Ureña-López L.A., 2003, *Phys. Rev. D*, 68, 024023
- Harko T., 2011a, *MNRAS*, 413, 3095
- Harko T., 2011b, *JCAP* 1105:022
- Harko T., Madarassy E. J. M., 2011, arXiv:1110.2829v1
- Hu Wayne, Barkana R., Gruzinov A., 2000, *Phys. Rev. Lett.*, 85, 1158
- Ji S. U., Sin S. J., 1994, *Phys. Rev. D*, 50, 3650
- Klypin A., Kravtsov A. V., Valenzuela O., Prada F., 1999, *ApJ*, 522, 82
- Kormendy J., Freeman K. C., 2004, in Ryder S. D., Pisano D. J., Walker M. A., Freeman K. C., eds, *IAU Symp.* . 220, *Dark Matter in Galaxies*. Cambridge Univ. Press, Cambridge, p. 377
- Kuzio de Naray R., McGaugh S.S., de Blok W.J.G., 2008, *ApJ*, 676, 920
- Lahav O., Liddle A.R., 2010, arXiv:1002.3488v1
- Lora V., Magaña J.A., Bernal A., Sanchez-Salcedo F. J., Grebel E. K., 2011, arXiv:1110.2684
- Matos T., Guzmán F. S., 2001, *Class. Quantum Grav.*, 18, 5055
- Matos T., Ureña-López L. A., 2001, *Phys Rev. D*, 63, 063506
- Matos T., Vazquez A., Magaña J.A., 2009, *MNRAS*, 389, 13957
- McGaugh S. S. et al., 2001, *ApJ*, 122, 2381
- Milgrom M., 2010, *AIP Conf.Proc.* 1241:139 arXiv:0912.2678v2
- Navarro J. F., Frenk C. S., White S. D. M., 1996, *ApJ.*, 462, 563
- Navarro J. F., Frenk C. S., White S. D. M., 1997, *ApJ*, 490, 493
- Navarro J.F. et al., 2010, *MNRAS*, 402, 21
- Oh Se-Heon, Brook Chris et al., 2011, arXiv:1011.2777v2.
- Peebles P.J.E., Lyman A.P. Jr., Bruce R.P, *Finding the Big Bang*, Cambridge University Press 2009
- Rindler-Daller T., Shapiro P. R., 2011, arXiv:1106.1256v2
- Robles V.H., Matos T., 2011, in preparation.
- Sanders R. H., 2009, *Adv. Astron.*, 2009, Article ID 752439, 9 pages.
- Sin S. J., 1994, *Phys. Rev. D*, 50, 3650
- Spano M. et al., 2008, *MNRAS*, 383, 297
- Suárez A., Matos T., 2011, *MNRAS*, 416, 87
- Zinner N. T., 2011, arXiv:1108.4290v1